Journal of Engg. Research Vol. 7 No. (1) March 2019 pp. 1 - 17

Strength properties of roller compacted concrete containing GGBS as partial replacement of cement

Sorabh Saluja*[1], Shweta Goyal* and Bishwajit Bhattacharjee**

**Department of Civil Engineering, Thapar Institute of Engineering and Technology, Patiala, 147004, India*
***Department of Civil Engineering, Indian Institute of Technology, HauzKhas, New Delhi- 110016, India*
**(1) Corresponding Author:sai1983saluja@gmail.com*

ABSTRACT

The present research is aimed to achieve zero slump concrete (roller compacted concrete) in laboratory environment by using soil approach. Roller compacted concrete (RCC) consists of a mixture of cementitious materials, sand, dense graded aggregates, and water. RCC is used mainly for heavy duty pavement and a variety of industrial applications. Different RCC mixtures were prepared for 0%, 20%, 40%, and 60% replacement of ordinary Portland cement (OPC) with ground granulated blast furnace slag (GGBS). Optimum water content of each mix was finalized after conducting compaction test for each replacement level. Strength and micro-structural properties of RCC mix modified with GGBS were investigated. The resultant properties are discussed in light of stoichiometric analysis of concrete with cementitious materials. The results indicate that RCC mix containing GGBS gives lower early age strength as compared to normal OPC concrete and the strength of GGBS mixes improves with age and provides higher compressive strength compared to normal OPC concrete. Further, the test results show that strength properties of RCC mixture containing GGBS increase upto 40% replacement level of OPC with GGBS. SEM morphology also shows dense, compact and uniformly spread C-S-H gel in RCC mix containing 40% GGBS.

Keywords: GGBS; optimum moisture content; RCC; soil compaction; stoichiometric analysis.

Abbreviation:

RCC: roller compacted concrete

GGBS: ground granulated blast furnace slag

γdry: dry density

γwet : wet density

(OH): hydroxyl ions

CH or $Ca(OH)_2$: calcium hydroxide

C-S-H: calcium silicate hydrate

C_3S: tricalcium silicate (alite)

C_2S: dicalcium silicate (belite)

C_3A: tricalcium aluminate (celite)

C_4AF: tetra calcium aluminoferrite (brownmillerite)

C_3AH_6: tricalcium aluminate hydrate (hydrogarnet).

INTRODUCTION

Roller compacted concrete (RCC) is a zero-slump concrete known for its economy, strength, and fast placement (ACI 325.10R-95, 2001; ACI 207.5R, 1988). The constituents of RCC are similar to those of conventional concrete and the construction and placement procedure is similar to asphalt pavement (Rao et al., 2016). RCC has seen increased utility in the past few decades, primarily due to its cost efficiency, and ease of handling during transport and

placement of concrete. In RCC pavement construction, formwork, reinforcing steel, and dowel bars are not required, which decreases the overall construction cost of the pavement. Further, the transverse cracking in RCC pavements is prevented through the denser particle structure leading to good aggregate interlock and interlock with the subbase interface (Zollinger, 2016).

In comparison with conventional concrete, to attain the same compressive strength RCC requires 20-28% less cementitious material (Hesami et al., 2016; Vahedifard et al., 2010). It has been widely used in concrete gravity dams because of lower heat of hydration as compared to conventional concrete. Additionally, low water-cement ratio in RCC leads to lesser cement paste in the concrete matrix, thus leading to less shrinkage and lower bleed water, which reduces the possibility of producing cracks than in conventional concrete. Besides dam and pavement construction, RCC has been used for wide variety of applications such as log sorting yards, lumber storage, forestry and mining haul roads, military vehicle roads and parking areas, bulk commodity storage areas, truck and automobile parking, municipal streets, secondary highways, airfield, and airport transportation (ACI 325.10R-95; Yazici et al., 2015).

The basic constituents of RCC are cementitious materials, dense-graded aggregates, and water. Since a relatively smaller amount of water is used in RCC, the resultant mix is super dry and cannot be placed by the general conventional (slump) concrete method. The compaction of the mix is carried out by vibratory rollers. The maximum size of coarse aggregates used in RCC varies depending on its application in dams or in pavement, with the smaller size aggregates used in later applications. Apart from the conventional building materials, the use of various mineral admixtures such as micro-silica fume, fly ash, and ground granulated blast furnace slag (GGBS) helps in reducing the cost of RCC further and improves the resultant properties of the mix (Cao et al., 2000; Atis et al., 2004; Rao et al., 2016; Aghabaglou and Ramyar, 2013). GGBS is a by-product from blast furnace used to make iron, and the amount of iron and slag produced is of the same order (Oner and Akyuz, 2007). GGBS is a mixture of alumina, silica, magnesium oxide, and lime, which is present in Portland cement but in different proportion.

LITERATURE REVIEW

Industrial waste like fly ash, bottom ash, GGBS, metakaolin, etc. is released from various industries in huge amounts. These industrial waste poses various difficulties in their disposal. To overcome these waste management issues, the best solution is to utilize these waste products in construction industry. Apart from reducing the overall cost of the project, the addition of industrial by-products increases the overall compressive strength of concrete. Inclusion of micro-silica further reduces the permeability of concrete.

The use of these industrial by-products for RCC production has been exploited by various researchers. Cao et al. (2000) investigated the effect of high volume fly-ash (HFRCC) on compressive and flexural strength of RCC. They observed that early age strength of HFRCC was poor, while long curing age strength was more remarkable. Atis et al. (2004) studied the efficiency of using fly ash in RCC in terms of improvement in strength properties of the resultant mix. Mix containing 15% fly ash as replacement to cement registered higher compressive strength than the control mix, while strength comparable to the normal Portland cement was observed at 30% replacement levels of cement. Atis (2005) further investigated the strength characteristics of RCC mixes made with two different low lime Class F fly ashes, namely, Drax and Aberthaw, as cement replacements under moist and dry curing conditions. It was observed that the type of fly ash has large influence on properties of the mix. It was reported that Drax fly ash at 50% replacement level gives 8.4% higher compressive strength on comparison with normal Portland cement under dry curing conditions. On the other hand, low quality fly ash (Aberthaw) presents lower compressive strength at both 50% and 70% replacement levels of cement with fly ash. Vahedifard et al. (2010) studied the effect of the addition of silica fume and Pumice on fresh and hardened properties of low cement RCCP mixture. They observed that the mix with 10% silica fume has higher compressive strength as compared to the control mix with a slight decrease in workability of fresh concrete. On the other hand, the use of pumice helped in making the mix more workable but it decreases the compressive strength. Srivastava et al. (2014) recommended the optimum dose of replacement of OPC with silica fume as 5%. At this replacement level silica fume inclusion increases both the workability and strength of the concrete. Aghabaglou and Ramyar (2013) studied the mechanical properties of RCC made with fly ash, used as

a replacement to both cement and fine aggregates. They observed that the increased content of cement replacement with fly ash causes reduction in strength, while fine aggregates replacement with fly ash gives the higher strength over the control mix. Hesami et al. (2016) investigated the effect of coal waste powder, coal waste ash, and lime stone on the strength properties of RCC pavement and observed that 5% replacement level shows the equivalent performance to the control mix. Rao et al. (2016) investigated the strength and abrasion resistance of RCC made with fly ash and manufactured sand (M-sand). They replaced the cement with fly ash at replacement level of 0%, 20%, 40%, and 60% along with the fine aggregates replacement with M-sand. They observed that the combined effect of M-sand and fly ash shows better performance.

Some of the researchers investigated the effect of GGBS as a replacement of cement for conventional concrete. Although GGBS tends to decrease the early age strength of concrete, it improves the workability, later age strength, and durability of the conventional concrete (Swamy and Bouikni, 1990; Liu et al., 2014; Chidiac and Panesar, 2008). Babu and Kumar (2000) studied the effectiveness of GGBS in normal concrete with cement replacement levels varying from 10% to 80%. Li and Zhao (2003) studied the effect of fly ash and GGBS on compressive strength and resistance to H_2SO_4 attack. They observed that the combination of fly ash and GGBS improves both fresh and hardened properties of concrete, while larger replacement of cement with fly ash requires relatively longer time to get beneficial results. Oner and Akyuz (2007) studied the optimum usage of GGBS for compressive strength of concrete. They observed that 55 -59% replacement level of total binder with GGBS gives the maximum strength. Liu et al. (2014) studied the effect of composite mineral admixture, steel slag, and GGBS with four different GGBS to steel slag ratios on mechanical and durability properties of concrete. They observed that composite mineral admixture and steel slag having higher amount of steel slag have adverse effects on the strength and durability properties of concrete, while GGBS improved the long term properties of concrete.

While an extensive research has been carried out on the utilization of GGBS in conventional concrete, limited research work has been reported on its effect when used for making RCC. Rao et al. (2016) investigated the strength properties and abrasion resistance of RCC made with GGBS. Mix proportions for all RCC mixes adopted by them are based upon flexural strength of 5 MPa according to ACI 211.3R (2002) guidelines. They reported that the maximum strength of the RCC mix is achieved at 40 % replacement level of cement with GGBS; however, the strength of GGBS mixes was reported to be higher than that of the control mix, even at 60% replacement level.

The aim of the present research is to achieve the zero slump concrete for the replacement of cement with various percentages of GGBS by using soil compaction approach. In the compaction approach, voids in the paste are minimized by achieving maximum dry density, which ultimately reduced the cement and water requirement. This approach is comparable to the field application of RCC in pavements since the compaction applied by surcharge in laboratory can correspond to the effort applied by the rollers in the field. Also, the influence of GGBS on long term strength properties of RCC was studied by making the number of RCC mixture with different amount of GGBS and studying the properties of the mix till 365 days of casting.

EXPERIMENTAL DETAILS

Materials

The cementitious materials used in the present study were Ordinary Portland cement (OPC) satisfying BIS: 8112-1989 (2005) and GGBS conforming to BIS: 12089-1987 (2004) as binders. The chemical composition and physical properties of cement and GGBS are presented in Table 1. The slag activity index of GGBS was 1.73. The coarse aggregate used was crushed gravel with nominal maximum size of 20 mm and 10 mm. The specific gravity and water absorption of 10 mm aggregate were 2.65 and 1.4% and for 20 mm aggregate, 2.63 and 1.38%, respectively. The fine aggregate used was river sand conforming to Zone-II with water absorption, specific gravity, and fineness modulus as 1.8%, 2.70, and 3.14, respectively.

Table 1. Chemical and Physical properties of Cement and GGBS.

Properties	SiO_2 (%)	Al_2O_3 (%)	Fe_2O_3 (%)	CaO (%)	MgO (%)	SO_3 (%)	Na_2O (%)	K_20 (%)	LOI	Specific gravity	Fineness (m^2/kg)
Cement	20.68	4.87	3.35	62.13	1.73	2.43	0.21	0.69	1.94	3.12	305
GGBS	31.6	21.7	2.5	33.2	8	0.18	0.85	-	0.98	2.83	385

RCC mixture composition

As for the conventional concrete mix designs, many methods are available for the RCC mix design also. In the present research, soil compaction philosophy was used to determine the mixture proportion for RCC. According to this philosophy, for a specified solid content of material, the aim is to determine the optimum moisture content for a laboratory compaction effort. The compaction applied by surcharge in laboratory corresponds to the effort applied by the rollers in the field. As per ACI 211.3R-02 (2002), initially the proportion of the aggregate to be used is finalized. Thereafter, the cementitious material content and water are decided by the optimum moisture content method described in ASTM D 1557 (2009). The step wise procedure is discussed in details in the following sections.

Proportioning of aggregates

Aggregates composition used in RCC mixture was selected so as to create dense-graded combined aggregates curve as per ACI 211.3R-02 (2002). Various types of combinations of fine aggregates, 10 mm aggregate, and 20 mm aggregate were tried and the combined aggregate curve was obtained. The aggregates grading curve corresponding to a combination of 55% of fine aggregate, 30% of 10 mm coarse aggregate, and 15% of 20 mm coarse aggregate was dense-graded and within the limits prescribed by ACI 211.3R (2002). The resultant grading curve is presented in Figure1.

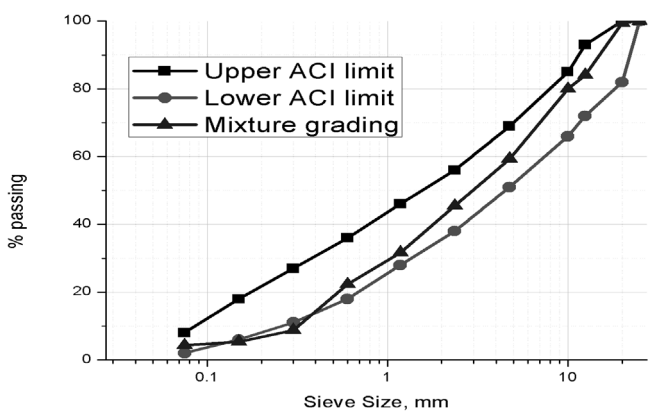

Figure 1. Gradation curve for combined aggregates and ACI limits.

Determination of cement and water content

After finalizing the aggregates, the cementitious material content and water was to be decided. According to ACI 211.3R (2002), the cementitious materials for RCC pavement range from 10 to 17% of the total dry mass of coarse and fine aggregates depending on strength and durability requirements. In the present study, cementitious materials were varied from 11% to 17% in various trail mixes and the optimum moisture content of each mix was finalized by using ASTM D 1557 (2009).

According to ASTM D 1557 (2009), moisture content of the mix was determined by compaction test conducted at an increment of water content. In the present study, method B of ASTM D 1557 (2009) was used for compaction test. In this test, 100 mm diameter mold having volume 920.89 cm^3 was used and the RCC material was compacted using a mechanical rammer–circular face having 4.537 kg weight. The material was compacted in five layers with 25 blows per layer.

For each mix, after finalizing the dry ingredients, moisture-density specimens were prepared by varying the water content. For initial trial mixes without GGBS, the water content variation was 5%, 5.5%, 6%, 6.5%, and 7% of total dry mass of RCC mixture. The material was mixed and compacted as stated earlier and the wet mass of the compacted concrete was noted. Along with that, the oven dry mass of the specimen was also obtained by drying the specimen in the oven for 24 hours at 100°C. The data was used to measure water content (w) and dry density (γdry) according to equations (1) and (2), respectively (Aghabaglou and Ramyar, 2013),

$$w(\%) = \frac{\mathrm{m}_{wet} - \mathrm{m}_{dry}}{\mathrm{m}_{dry}} \mathrm{x}\, 100 \qquad \text{eq. (1)}$$

$$\gamma_{dry} = \frac{\gamma_{wet}}{1+\mathrm{w}} \qquad \text{eq. (2)}$$

where mwet corresponds to wet mass of the sample, mdry corresponds to oven dry mass of the sample, w is the water content (%), γdry is the dry density of the sample, and γwet is the wet density of sample.

A graph between moisture content and density was then prepared for the control mix. The peak point in the moisture–density curve is taken as the optimum moisture content for the mix. Various mixes with 11 to 17% cement content were then cast and based on the 28 days compressive strength; the mix with 16% of cement as total dry mass of coarse and fine aggregate was taken as the control mix.

For evaluating the influence of GGBS on the strength properties, various RCC were made by using GGBS as cement replacement at the level of 20%, 40%, and 60% by weight. In all these mixes, cementitious content was kept constant as decided for the control mix. The moisture content-density curves were prepared for each replacement level and optimum moisture content was finalized. The curves obtained for the finalized mixes are presented in Figure 2.

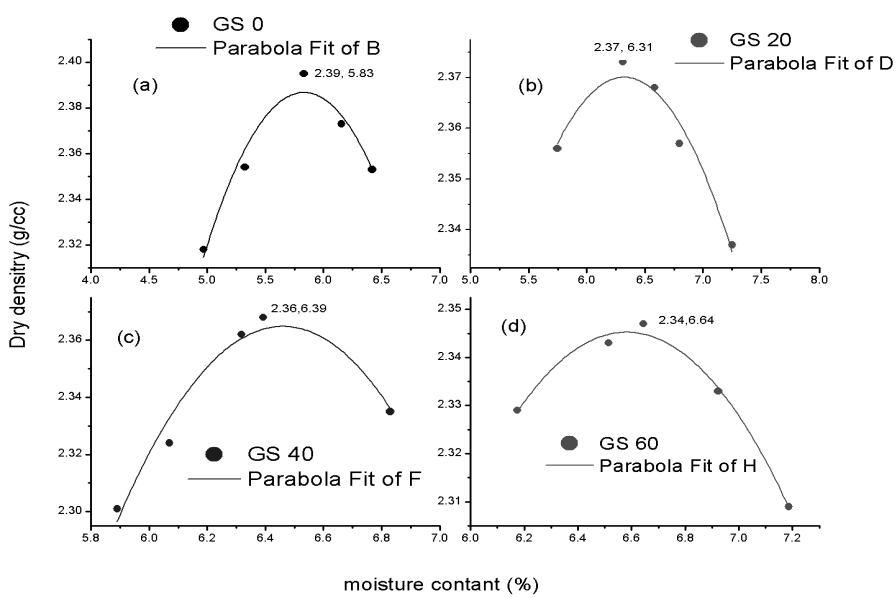

Figure 2. Relation between maximum dry density and optimum moisture content for (a) GS 0, (b) GS 20, (c) GS 40, and (d) GS 60, respectively.

After finding the optimum moisture content corresponding to each mix, the RCC mix proportions were finalized as per ACI 211.3R (2002). Table 2 presents the RCC mix proportions finalized for the present study. Table 2 clearly shows that water content increases with the increase in GGBS content of the mix.

Sample preparation

The test specimens consisted of (a) 150 x 300 mm cylinders for determination of compressive strength and split tensile strength and (b) 150 x150 x700 mm prisms to evaluate flexural strength.

Table 2. RCC mix proportion utilized in the present study.

Mix No.	Cementitious materials (kg/m^3)		Water (kg/m^3)	w/cm	Sand (kg/m^3)	Aggregate(kg/m^3)	
	Cement	GGBS				10 mm	20 mm
GS 0	327.87	0	119.30	0.36	1127.06	614.76	307.38
GS 20	259.38	64.85	127.86	0.39	1114.51	607.92	303.96
GS 40	193.65	129.10	129.10	0.40	1109.46	605.16	302.58
GS 60	128.14	192.22	133.04	0.42	1101.23	600.67	300.34

The RCC mixture was made in a rotating mixture keeping 5 min mixing time. To achieve complete compaction, a vibrating table with a vibration frequency of 60 Hz specified in ASTM C 1170 (2008) was used. The RCC was filled into the molds in three layers and compacted by putting surcharge on the top of each layer. According to ASTM C 1176 (2008), for cylindrical samples 4.9 kPa (9 kg) surcharge was used to facilitate consolidation as shown in Figure 3(a). For prism specimens no standard was available; therefore the surcharge was kept as 4.9 kPa (54 kg) for proper consolidation (Figure 3(b)). The dimensions of the surcharge were kept smaller than the inside dimension of the corresponding molds. All the specimens were consolidated till the formation of mortar ring between the inside face of the mold and the surcharge. The formation of this mortar ring shows that the RCC has reached its maximum density.

After 24h of casting, all the specimens were de-molded and kept in curing tank having temperature 25 ± 2°C and 100% relative humidity. Compressive strength tests were conducted at 7, 28, 60, 90, and 365 days of curing as per BIS: 516-1959 (2004). Split tensile strength and flexural strength tests were conducted at 7, 28, 90, and 365 days of curing as per BIS: 516-1959 (2004). A total of 108 cylinders and 48 prisms specimens were made and tested for the present study.

(a) **(b)**

Figure 3. Preparation of (a) cylindrical and (b) beam shaped specimens.

RESULTS AND DISCUSSION

Optimum moisture content

Figure 4 shows the resultant curves for optimum water content and maximum dry density for all four mixtures. Table 3 shows optimum water content and maximum dry density achieved by compaction test. It was observed that the increase in GGBS content results in an increase in the optimum water content.

Table 3. Optimum water content, maximum dry density of the RCC mixture.

RCC Mix	Mix designation	Optimum water content (%)	Maximum dry density (g/cc)	Equation between dry density (y) and water content (x)	R^{2*}
100% OPC +0% GGBS	GS 0 (control)	5.833	2. 395	$Y= -0.09x^2+1.13x-0.91$	0.953
80% OPC + 20% GGBS	GS 20	6.310	2.373	$Y= 0.04x^2+0.50x+0.77$	0.963
60% OPC + 40% GGBS	GS 40	6.393	2.368	$Y= -0.21x^2+2.71x-6.40$	0.961
40% OPC + 60% GGBS	GS 60	6.644	2.347	$Y= -0.09x^2+1.31x-1.96$	0.990

* Coefficient of determination index.

Aghabaglou and Ramyar (2013) found that this increase trend may be due to higher fineness of GGBS as compared to cement. Further, lower specific gravity of the GGBS as compared to cement results in a decrease in dry density of RCC. Figure 4 shows that the optimum water content of RCC mixture decreased with the increase in maximum dry density. A similar finding was also observed by Yazici et al. (2015); Aghabaglou and Ramyar (2013); Hesami et al. (2016).

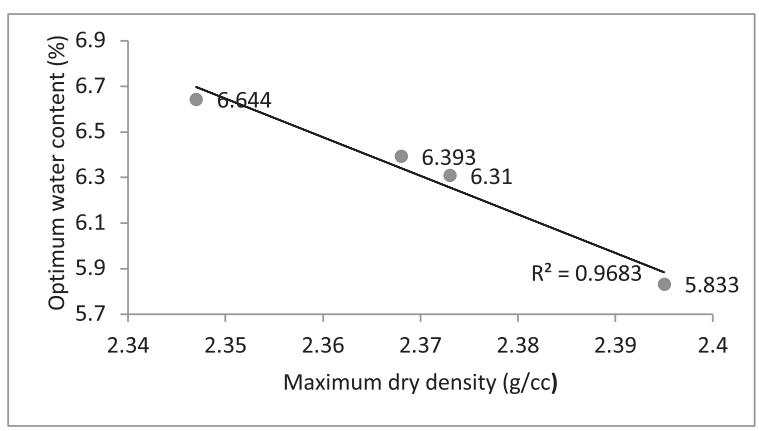

Figure 4. Relationship between optimum water content and maximum dry density for all RCC mixture.

Compressive Strength

Figure 5 presents the compressive strength results of RCC mixture at testing ages of 7, 28, 60, 90, and 365 days. The result shown in Figure 5 was corresponding to the average of the three samples' results conducted on each mixture. At 28 days, all RCC mixes had compressive strength higher than the minimum value of 27.6 MPa required for RCC to be used as surface course as specified in ACI 325.10R (2001).

At 28 days, the observed compressive strength of control RCC sample (GS0) was highest, indicating that the contribution of GGBS to the strength development was smaller compared to OPC. A similar observation of lower 28-day strength of conventional concrete incorporating GGBS was made by Liu et al. (2014); Li and Zhao (2003). However, Oner and Akyuz (2007) recommended that, in conventional concrete, 55-59% replacement level of the total binder with GGBS gives the maximum strength. The authors in their research fixed the cement content and added additional GGBS into the mix proportions, which ultimately reduce the aggregates proportions; i.e., the cement content was not reduced with the GGBS additions.

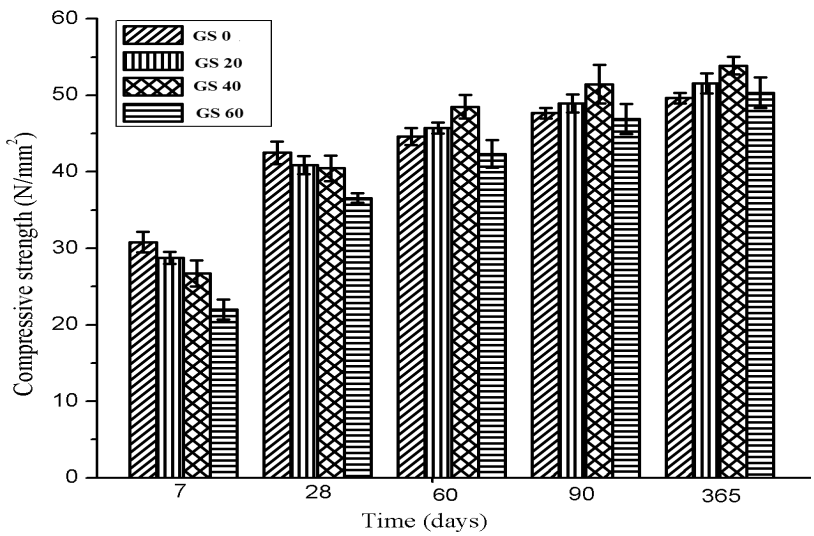

Figure 5. Compressive strength variation of all RCC mixture.

Beyond 28 days, the presence of GGBS was observed to be highly advantageous at 20 % and 40% replacement level with a strength exceeding the corresponding control RCC mix, while 60% replacement level gives slightly lower compressive strength as compared to GS 0 mix at 90 days of testing. However, the strength of GS 60 mix improved with the curing duration and 365 days compressive strength of the mix was found to the slightly higher than the corresponding control mix. The strength development rate was found to be higher in GGBS mixes. The strength development rate from 28 days to 365 days was found to be highest in GS 60 (37.6%), while GS 0 mix had the smallest strength gain of 16.8%. In mix GS 20 and GS 40, strength gain observed was 26.1% and 33.1%, respectively. Results indicate that GGBS percentage and curing age had a great effect on compressive strength development. The glossy components in GGBS react gradually with water and therefore, the secondary pozzolanic reaction between GGBS and (OH) ions produced during hydration of cement is slow. Further, at large replacement levels of GGBS, the whole of GGBS does not get consumed in the pozzolanic reaction due to lesser availability of $Ca(OH)_2$ from primary hydration reaction. It indicates that, at 60% replacement level, GGBS cannot be used effectively as a binder; rather it works as filler in the concrete.

To study the microstructure behavior of RCC, fractured small size pieces of compressive strength specimens were taken and used for Scanning Electron Micrographs (SEM) analysis. SEM gives the information regarding the topographic and compositional behaviour of the material. In the present research work, fractured small pieces of the specimens were mounted on the SEM stub and images were obtained using SE image mode. SEM images for control RCC (GS 0) mix and for RCC containing 40% GGBS (GS 40) are shown in Figure6.

As can be observed from Figure 6(a), GS 0 mix has a large number of hexagonal structures of calcium hydroxide at 28 days of curing. For RCC containing 40% GGBS (GS 40), C-S-H gel becomes more visible as can be seen in Figure 6(b). However, the C-S-H gel so formed is porous in structure. It clearly indicates that the calcium hydroxide crystals get converted into C-S-H gel due to secondary pozzolanic reaction. Less monolithic behavior of C-S-H gel may be due to partial reaction of GGBS with water and the presence of glossy slag parcels at this stage of curing. With the increase in curing time till 90 days, GS40 mix has highly dense structure with large amount of C-S-H gel and negligible pores (Figure 6(c)).

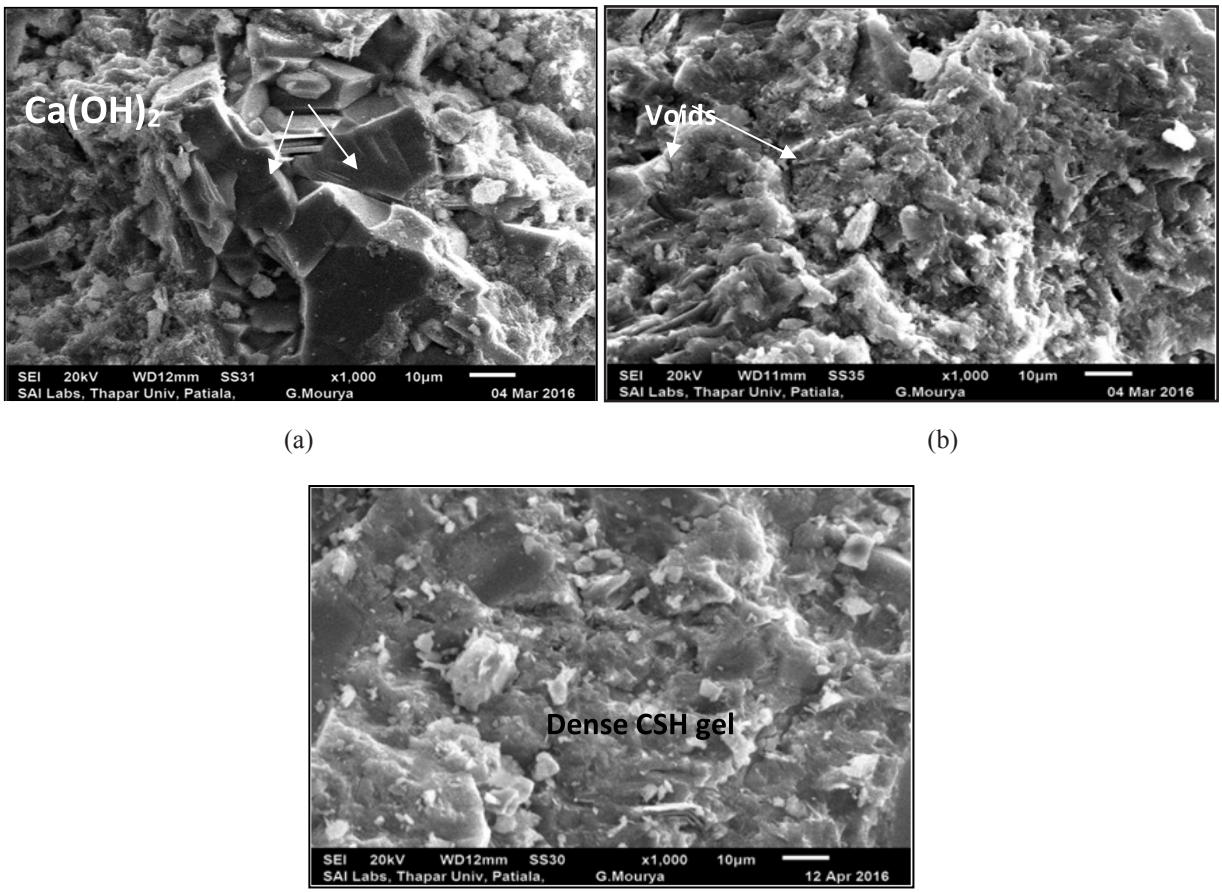

Figure 6. Scanning Electron Morphology of (a) GS 0 mix at 28 days, (b) GS 40 mix at 28 days, and (c) GS 40 mix at 90 days of curing age.

Split tensile strength

Figure7 shows the split tensile strength of the various RCC mixtures. At early curing age of 7 days, in GS 20, GS 40, and GS 60 mix, 33.6%, 30.9%, and 29.2% decrease in split tensile strength were observed over the control (GS 0) mix. The above difference in split tensile behavior was dropped to 24.5 % and 7.2% for GS 20 and GS 60, respectively, while in GS 40 mix, 2.2% increase was observed at 28 days of curing age. GS 40 and GS 60 mix show significant increase in split tensile strength after 28 days of curing. At 365 days of curing, the increase in split tensile strength for GS 40 and GS 60 over that of GS 0 mixture was 26.6% and 21.7%, respectively. The observed behaviour shows that the addition of GGBS in concrete improved the splitting tensile strength of concrete after 28 days of curing age. GGBS affects the splitting tensile behavior different than the compressive strength behavior. The split tensile strength of concrete is affected with the quality of paste and interfacial transition zone in the concrete. The fineness and pozzolanic properties of GGBS improve the quality of paste at later ages of curing, which results in an increase in split tensile strength of RCC. Observed behavior for split tensile strength is in good agreement with those reported by Atis et al. (2004) and Cao et al. (2000). To use RCC in pavement, according to ACI 325.10R-95 splitting tensile strength range at 28 days is 2.8 to 4.1 MPa. All RCC mixture satisfied the limit at 28 days of age.

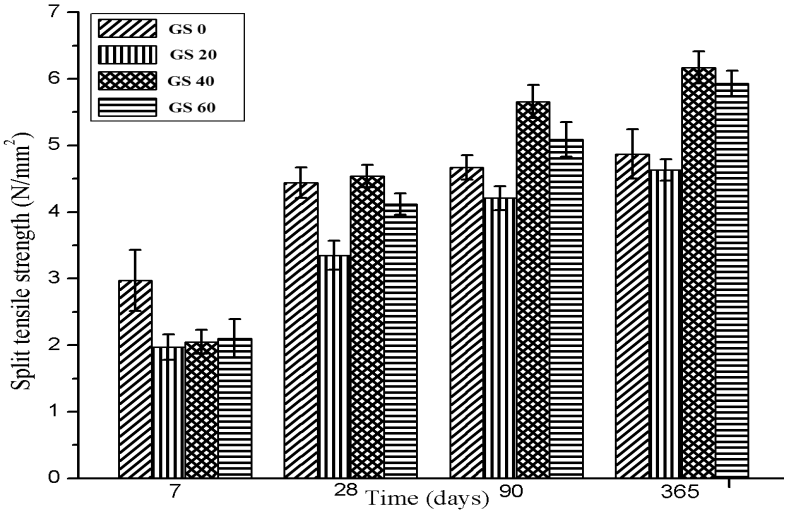

Figure 7. Split tensile strength variation of all RCC mixture.

Flexural strength

Figure 8 presented the flexural strength results for all RCC mixtures. From Figure 8 it was seen that flexural strength of RCC mixture containing GS20, GS40, and GS60 decreased by 28.8%, 31.86%, and 43.43% of flexural strength of GS0 mix at 7 days of curing. RCC containing 20% and 60% GGBS shows a decrease in flexural strength as compared to control RCC mix at all curing ages. Similar to compressive strength results, 40% GGBS gives the higher flexural strength at 365 days of curing. In RCC mixture containing GS 20 and GS 60, a decrease in the flexural strength observed was 6.9% and 13.3%, respectively, while in GS 40 RCC mix, 5.45% increase in strength was observed at 365 days of curing. Flexural strength gain from 28 days to 365 days in mix GS0, GS20, GS40, and GS60 observed was 23.84%, 33.40%, 43.18%, and 41.20%, respectively. It can be concluded that increasing the replacement level of cement with GGBS results in a percentage increase in strength. The previous studies also show that the pozzolanic reactions of GGBS are slow during the initial age of curing (28 days) after this period; the GGBS starts reacting with calcium hydroxide and forms CSH gel. Calcium hydroxide was formed after the hydration of cement so that it takes longer time to develop its strength particularly at high GGBS replacement level (Zhou et al., 2012).

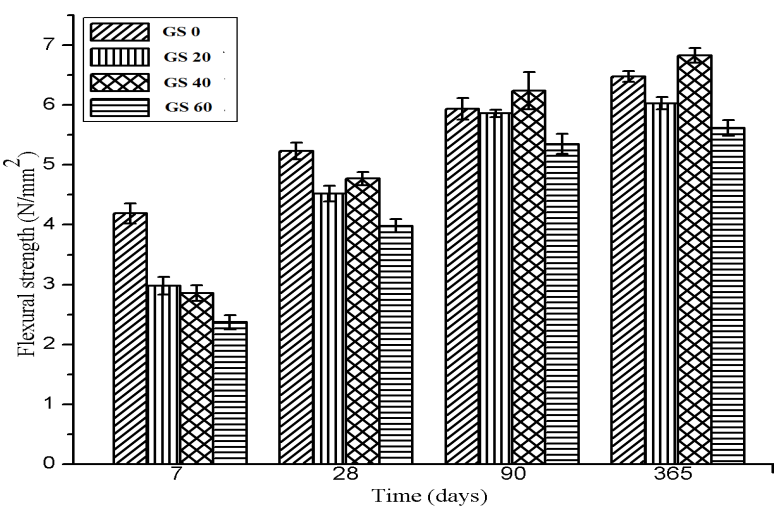

Figure 8. Flexural strength variation of all RCC mixture.

It was observed that the RCC mixture containing 40% GGBS gained a higher compressive strength, split tensile strength, and flexural strength as compared to control RCC mix after 28 days of curing. After 28 days of curing age, pozzolanic effect of GGBS overcome all the negative effects and enhanced the strength properties of RCC mixture. However, all mechanical strengths of the RCC mixture decreased at 60% replacement level. This clearly indicates that there is an upper limit of the level of substitution of cement by GGBS. The upper limit can be correlated with the chemical composition of cement and GGBS on the basis of stoichiometric analysis.

Stoichiometric analysis

The stoichiometric analysis of cement hydration involves reaction of cement compounds in the presence of water. The major compounds of Portland cement arealite, belite, celite,and brownmillerite. The phase compositions of these compounds are mostly found by Bogue equation, which is based on the chemical composition of cement (Prochon and Piotrowski, 2016). The basic Bogue equations for calculation of cement compounds are as follows (Prochon and Piotrowski, 2016):

C_3S (alite): $4.07\ CaO - 7.6\ SiO_2 - 6.72\ Al_2O_3 - 1.43\ Fe_2O_3$ eq.(3)

C_2S (belite): $2.87\ SiO_2 - 0.75\ C_3S$ eq. (4)

C_3A (celite): $2.65\ Al_2O_3 - 1.69\ Fe_2O_3$ eq. (5)

C_4AF (brownmillerite): $3.04 Fe_2O_3$ eq. (6)

On the basis of chemical composition of cement used in the present study (Table 1), the phase composition of various cement compounds, viz., C_3S, C_2S, C_3A, and C_4AF is obtained as 58.19%, 15.71%, 7.24%, and 10.18%, respectively. In addition to these major compounds, some minor compounds such as MgO, SO_3 and Na_2O are present, which together are taken as 8.67%.

The basic stoichiometric equations of hydration of the major cement compounds can further be summarized as follows (Neville, 2012):

For C_3S: $2C_3S + 6\ H \longrightarrow C\text{-}S\text{-}H + 3CH$ eq. (7)

C_2S: $2C_2S + 4H \longrightarrow C\text{-}S\text{-}H + CH$ eq. (8)

C_3A: $C_3A + 6H \longrightarrow C_3AH_6$ eq. (9)

C_4AF: $C_4AF + 2CH + 10H \longrightarrow C_6AFH_{12}$ eq. (10)

On the basis of atomic masses, it can be observed that100 grams of C_3S and C_2S produces 49 grams and 22 grams of CH, respectively, and C_4AF consumed approximately 30 grams of CH. Therefore the stoichiometric equations for C grams of cement can be written as

For C_3S: $0.582\ C_3S + 0.139\ H \longrightarrow 0.436\ C\text{-}S\text{-}H + 0.285\ CH$ eq. (11)

C_2S: $0.157\ C_2S + 0.033H \longrightarrow 0.155\ C\text{-}S\text{-}H + 0.035\ CH$ eq. (12)

C_3A: $0.073\ C_3A + 0.029\ H \longrightarrow 0.102\ C_3AH_6$ eq. (13)

C_4AF: $0.102\ C_4AF + 0.031\ CH + 0.037 \longrightarrow 0.169\ C_6AFH_{12}$ eq. (14)

From the above stoichiometric equations, it was observed that C grams of cement produced 0.862 grams of C-S-H and 0.289 grams of CH after complete hydration.

Addition of GGBS into mix leads to alternation in hydration process. GGBS comprises higher quantities of SiO_2, Al_2O_3 and MgO, which promote the formation of hydrotalcite (M_5AH_{13}) and C-S-H (Stephantet al., 2015; Kolani et al., 2012). In mixtures containing GGBS, a secondary pozzolanic reaction occurs between CH liberated during the hydration of cement and silica component of GGBS. The stoichiometric equation for this secondary pozzolanic reaction corresponding to pure silica can be written as

$2S + 3CH \longrightarrow C_3S_2H_3$ eq. (15)

By considering the atomic masses of all the elements, it was observed that 1 part of silica would react with 1.851 parts of CH to produce 2.851 parts of CSH gel. The chemical composition of GGBS shows that it has 31.6% of silica in it. Therefore, one gram of GGBS will react with 1.851 × 0.316 (i.e.0.585 C) gram of CH to produce C-S-H gel. Since 0.289 C grams of CH is produced after complete hydration, it will require a maximum of 0.494 grams of GGBS for its conversion into CSH consumed during secondary pozzolanic reaction. Therefore, by stoichiometric analysis, the upper limit of substitution of cement by GGBS can be taken as 49.4%. Stoichiometric upper limits indicate that GGBS does not contribute towards strength development by chemical reactions beyond 50% replacement level, after which it will simply act as afiller.

The hydration reaction of a mix containing secondary cementation materials like GGBS can be termed as lime controlled or pozzolanic controlled based on the stoichiometric analysis. If the amount of CH produced by the hydration reaction is more than the amount that can be consumed by pozzolanic material present in the mix, the reaction is said to be pozzolanic controlled; and if CH produced is less than the amount required by the pozzolanic material, the reaction is said to be lime-controlled. The stoichiometric analysis of the RCC mixes used in the present study is presented in Table 4. It can be observed from the table that, till the 20% replacement of cement by GGBS, the reaction is pozzolanic-controlled and at 40% and 60% replacement level, the reaction becomes lime-controlled. In GS 40 mix the imbalance between the CH liberated and consumption during pozzolanic reaction was minimum. Therefore, GS40 mix is the most optimum mix in terms of theoretical CH consumption and in terms of strength development.

Table 4. Stoichiometry of hydration reaction for all mixes.

Mix Designation	Cement content (kg)	GGBS content (kg)	Maximum CH liberated (kg)	CH consumed by pozzolanic reaction (kg)	Amount of CH left/required	Limiting parameter
GS 0	327.87	0	94.76	-	94.76/--	Pozzolana
GS 20	259.38	64.85	74.96	37.94	37.02/--	Pozzolana
GS 40	193.65	129.10	55.96	75.52	--/19.56	Lime
GS 60	128.14	192.22	37.03	112.45	--/75.42	Lime

Relationship between mechanical properties

The correlation between compressive strength v/s split tensile strength, compressive strength v/s flexural strength, and flexural strength v/s split tensile strength is attempted for RCC. In the present work linear and power correlation between the strengths were investigated and presented in Figures 9 -11. Figure 9(a) shows the linear relation and Figure 9 (b) shows the power function between compressive strength and split tensile strength of RCC at 95% confidence interval. It was observed from the figure that a strong correlation exists between the split tensile and compressive strength of RCC. The correlation equations are as follows:

Linear function $f_s = 0.130 f_c - 1.302$ $R^2 = 0.869$ eq. (16)

Power function $f_s = 0.018(f_c)^{1.445}$ $R^2 = 0.906$ eq.(17)

where f_s is the split tensile strength (MPa), f_c is the compressive strength (MPa)

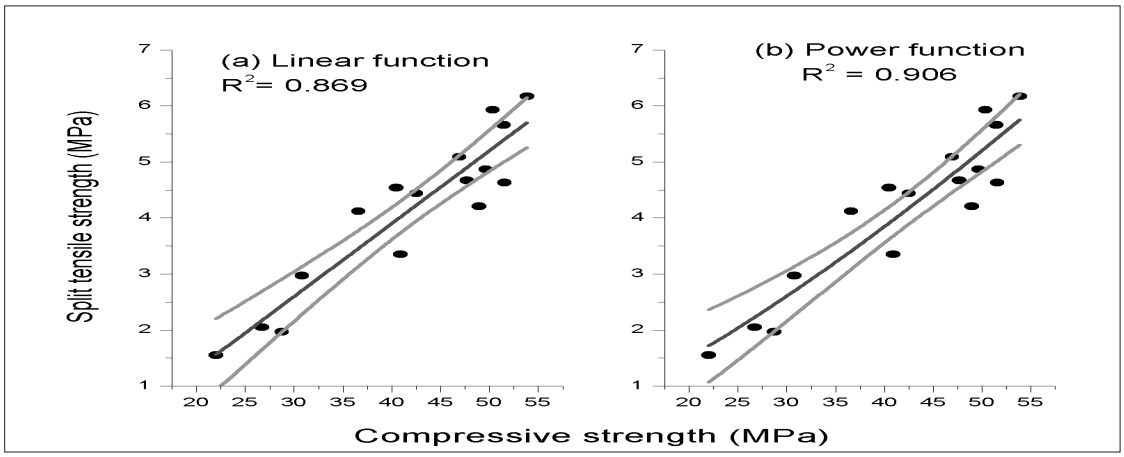

Figure 9. Relation between compressive strength and split tensile strength at 95% confidence interval.

Figure10 shows the relation between flexural strength and compressive strength at 95% confidence interval. It was observed that strong correlation coefficient (R^2) exists for power function (0.953) as well as for linear function (0.941). The correlation equations are

Linear function $f_{fl} = 0.131 f_c - 0.556$ $R^2 = 0.947$ eq. (18)

Power function $f_{fl} = 0.070(f_c)^{1.136}$ $R^2 = 0.953$ eq. (19)

Where f_{fl} is the flexural strength (MPa), and f_c is the compressive strength (MPa).

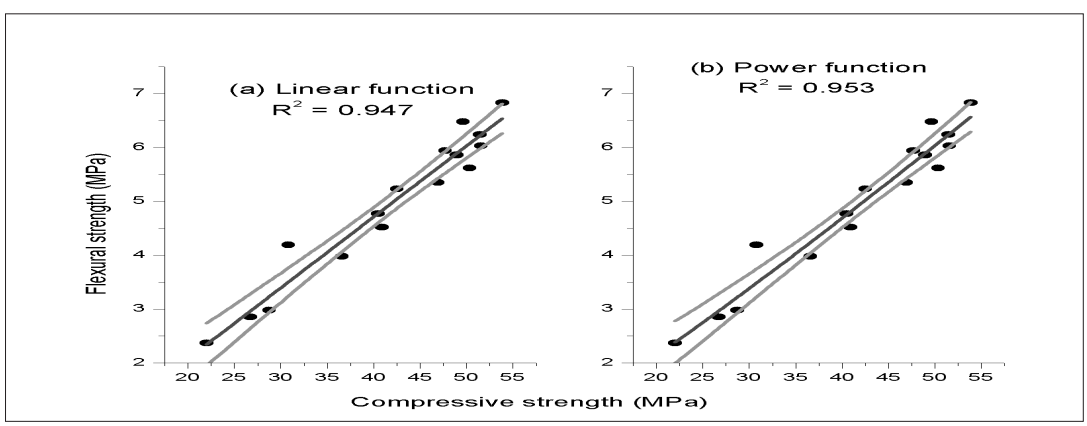

Figure 10. Relation between compressive strength and flexural strength at 95% confidence interval.

The relation between flexural strength and split tensile strength at 95% confidence interval was shown in Figure 11, and the correlation equations are:

Linear function $f_{fl} = 0.940 f_s - 0.517$ $R^2 = 0.830$ eq. (20)

Power function $f_{fl} = 0.565(f_s)^{1.233}$ $R^2 = 0.892$ eq.(21)

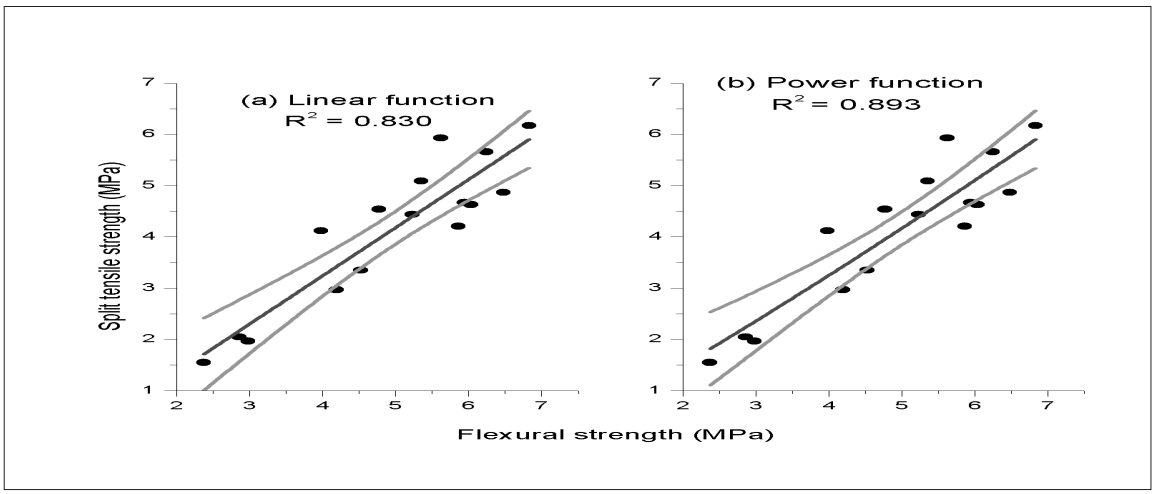

Figure 11. Relation between flexural strength and split tensile strength at 95% confidence interval.

Table 5 shows the statistical parameters including correlation coefficient (R^2), mean square error (MSE), and root mean square error (RMSE) calculated by using the above equations. It was noticed that power function has higher correlation coefficient (R^2) and lower mean square errors than the linear functions. The difference between R^2 and statistical errors is negligible except for the flexural strength v/s split tensile strength.

Most of the researchers (Rao et. al., 2016; Hesami et. al., 2016) correlate the relationship between mechanical properties in power format. However, the observed linear relationship between the mechanical properties also has a strong correlation and hence can be attempted for RCC mixes.

Table 5. Correlation coefficient (R^2), mean square error (MSE), and root mean square error (RMSE) of fitted functions.

Correlation relation between	Correlation equations between strength properties		Statistical Parameters		
	function	equation	R^2	MSE	RMSE
C.S. v/s S.T.S*	Linear	$f_s = 0.130 f_c - 1.302$	0.869	0.242	0.492
	Power	$f_s = 0.018(f_c)^{1.445}$	0.906	0.011	0.105
C.S. v/s F.S.	Linear	$f_{fl} = 0.131 f_c - 0.556$	0.947	0.092	0.303
	Power	$f_{fl} = 0.070(f_c)^{1.136}$	0.953	0.035	0.184
F.S. v/s S.T.S	Linear	$f_{fl} = 0.940 f_s - 0.517$	0.830	0.313	0.559
	Power	$f_{fl} = 0.565(f_s)^{1.233}$	0.892	0.007	0.084

***C.S:** Compressive strength; S.T.S: Split tensile strength; F.S: Flexural strength.

CONCLUSIONS

On the basis of obtained results, the following conclusions can be drawn:

1– RCC designed by compaction approach leads to minimum voids in mix with maximum density, which ultimately reduces the cement and water requirement.

2 – Addition of GGBS into the mix increases the water requirement to obtain a zero slump concrete.

3 – Optimum water content of RCC mixture decreases with the increase in maximum dry density.

4 – RCC mix containing GGBS has lower early age strength as compared to the corresponding control mix. However, as the curing time is extended, the rate of strength gain is higher in GGBS mixes. The rate of strength gain from 28 to 365 days is maximum for GS 60 mix (37.6%), followed by GS 40 (33.1%), GS 20 (26.1%), and GS 0 (16%).

5 – Maximum increase in all strength properties was observed in GS 40 mix as compared to the other RCC mixes at 90 and 365 days of curing. The increase in compressive strength, split tensile strength, and flexural strength for GS 40 mix is 8.5%, 26.6%, and 5.4% ,respectively, as compared to control mix (GS 0) at 365 days of testing.

6 – The improvement in strength properties of the mixes is further substantiated by stoichiometric equations of cement hydration in concrete. Stoichiometrically, the mix containing GGBS as 40% by replacement of cement is the most optimum mix in terms of CH consumption. SEM morphology also shows dense, compact, and uniformly spread C-S-H gel in RCC mix containing 40% GGBS.

7 – Strong correlation exists between various mechanical properties in power as well as in linear format.

8 – Improvement in strength properties with the replacement of cement with GGBS leads to an efficient use of natural resources and reduces the overall cost of the RCC construction without compromising the properties of RCC mix.

ACKNOWLEDGMENTS

The authors wish to express their gratitude to CountoMicrofine Products Pvt. Ltd., India, for supplying the GGBS for research work.

REFERENCES

ACI 207.5R, 1988. Roller compacted mass concrete. ACI material journal committee report. Tilte no. 85–M44.

ACI 211.3R -02, 2002. Guide for selecting proportions for No- slump concrete. American Concrete Institute.

ACI 325.10R -95, 2001. Report on roller-compacted concrete pavements. American Concrete Institute.

Aghabaglou, A.M. & Ramyar, K. 2013. Mechanical properties of high volume fly ash roller compacted concrete designed by maximum density method. Construction and Building Materials **38**:356–364.

ASTM C 1170/C1170M -08, 2008. Standard test method for determining consistency and density of roller compacted concrete using a vibrating table. American Society of Testing and Materials, Philadelphia.

ASTM C 1176/C1176 M -08, 2008. Standard practice for making roller compacted concrete in cylinder molds using a vibrating table. American Society of Testing and Materials, Philadelphia.

ASTM D15572009 ,09-. Standard test methods for Laboratory compaction characteristics of soil using modified efforts. American Society of Testing and Materials, Philadelphia.

Atis, C.D. 2005. Strength properties of high-volume fly ash roller compacted and workable concrete, and influence of curing condition. Cement and Concrete research **35**:1112–1121.

Atis, C.D., Sevim, U.K., Ozcan, F., Bilim, C., Karahan, O., Tanrikulu, A.H. & Eksi, A. 2004. Strength properties of roller compacted concrete containing a non-standard high calcium fly ash. Materials Letters **58**:1446–1450.

Babu, G.K. & Kumar, V.S.R. 2000. Efficiency of GGBS in concrete. Cement and Concrete Research **30**:1031–1036.

BIS 120891987-, Reconfirmed 2004. Specification for Granulated Slag for the manufacture of Portland Slag cement. Bureau of Indian Standards, New Delhi.

BIS 516 – 1959, Reconfirmed 2004. Indian Standard Methods of Tests for Strength of Concrete. Bureau of Indian Standards, New Delhi.

BIS 8112- 1989, Reconfirmed 2005. Specification for 43 Grade Ordinary Portland Cement. Bureau of Indian Standards, New Delhi.

Cao, C., Sun, W. & Qin, H. 2000. The analysis on strength and fly ash effect of roller-compacted concrete with high volume fly ash. Cement and Concrete research **30**:71–75.

Chidiac, S.E.& Panesar, D.K. 2008. Evolution of mechanical properties of concrete containing ground granulated blast furnace slag and effects on the scaling resistance test at 28days.Cement and Concrete Composites **30**(1): 63–71.

Hesami, S., Modarres, A., Soltaninejad, M. & Madani, H. 2016. Mechanical properties of roller compacted concrete pavement containing coal waste and lime stone powder as partial replacement of cement. Construction and Building Materials**111**:625–636.

Kolani, B., Lacarriere, L. B., Sellier, A., Escadeillas, G., Boutillon, L. & Linger, L. 2012. Hydration of slag blended cements. Cement and Concrete Composites **34**(9):1009–1018.

Li, G. & Zhao, X. 2003. Properties of concrete incorporating fly ash and ground granulated blast-furnace slag. Cement and Concrete Composites **25**:293–299.

Liu, S., Wang, Z. & Li, X. 2014. Long- term properties of concrete containing ground granulated blast furnace slag and steel slag. Magazine of Concrete Research **66**(21): 1095–1103.

Neville, A.M. 2012. Properties of Concrete (4th ed.). Dorling Kindersley Publishing, pp.12–30.

Oner, A. & Akyuz, S. 2007. An experimental study on optimum usage of GGBS for the compressive strength of concrete. Cement and Concrete Composites **29**:505–514.

Piotr, P. & Piotrowski, T. 2016. Bound water content measurement in cement pastes by Stoichiometric and gravimetric analyses. Journal of Building Chemistry, **1**:18–25.

Rao, S.K., Sravana, P. & Rao, T.C. 2016. Abrasion resistance and mechanical properties of roller compacted concrete with GGBS. Construction and Building Materials **114**:925–933.

Rao, S.K., Sravana, P. & Rao, T.C. 2016. Investigating the effect of M-sand on abrasion resistance of fly ash roller compacted concrete. Construction and Building Materials **118**: 352–363.

Srivastava, V., Kumar,R., Agarwal, V.C. & Mehta, P.K. 2014. Effect of silica fume on workability and compressive strength of OPC concrete. Journal of Environmental Nanotechnology **3**(2): 32–35.

Stephant, S., Chomat, L., Nonat, A. & Charpentier, T. 2015. Influence of the slag content on the hydration of blended cement. 14th international congress on the chemistry of cement, Beijing.

Swamy, R.N. & Bouikni, A. 1990. Engineering properties of slag concrete as influenced by mix proportioning and curing. ACI Material journal **87**:210–220.

Vahedifard, F., Nili, M. & Meehan, C.L. 2010. Assessing the effect of supplementary cementitious materials on the performance of low-cement roller compacted concrete pavement. Construction and Building Materials **24**:2528–2535.

Yazici, S., Tuyan, M., Mardani-Aghabaglou, A. & Ute, A.A. 2015. Mechanical properties and impact resistance of roller compacted concrete containing polypropylene fibre. Magazine of concrete research **67**(16):867–875.

Zhou, X.M., Slater, J.R., Wavell, S.E. & Oladiran, O. 2012. Effects of PFA and GGBS on early ages engineering properties of Portland cement systems. Journal of Advanced Concrete Technology **10**:74–85.

Zollinger, D. 2016. Roller compacted concrete pavement. FHWA–HIF–16–003, U.S. Department of Transportation.

SUBMITTED: 28/08/2017
REVISED : 25/02/2018
ACCEPTED : 08/03/2018

خـواص القـوة للخرسانة المضغوطـة بالمدحلـة التي تحتـوي على GGBS كبديل جـزئي للأسمنت

سورابه سالوجا * ، شويتا غويال * ، بيشواجيت بهاتاشارجي **

*قسم الهندسة المدنية، معهد ثابار للهندسة والتكنولوجيا، باتيالا، 147004، الهند

**قسم الهندسة المدنية، المعهد الهندي للتكنولوجيا، هوزخاس، نيودلهي، 110016، الهند

الخـلاصة

يهدف البحث الحالي إلى تحقيق خرسانة تتميز بنسبة انهيار صفر (الخرسانة المضغوطة بالمدحلة) في بيئة المختبر باستخدام نهج التربة. تتكون الخرسانة المضغوطة بالمدحلة (RCC) من خليط من المواد الأسمنتية والرمل وركام متدرج كثيف والماء. وتُستخدم هذه الخرسانة بشكل أساسي في عمليات الرصف الثقيل ومجموعة متنوعة من التطبيقات الصناعية. تم تحضير مخاليط مختلفة من الخرسانة المضغوطة بالمدحلة لاستبدال الأسمنت البورتلاندي العادي (OPC) بحبيبات خبث الفرن العالي المطحونة (GGBS) عند نسب 0 %، 20 %، 40 % و 60 %. تم صياغة المحتوى الأمثل للماء لكل خليط بعد إجراء اختبار الضغط لكل مستوى من مستويات الاستبدال. وتمت دراسة خصائص القوة والخصائص الهيكلية الدقيقة لخليط الخرسانة المضغوطة بالمدحلة المُعدل بإضافة GGBS. وتمت مناقشة الخصائص الناتجة في ضوء تحليل التكافوء الكيميائي للخرسانة مع المواد الأسمنتية. وأشارت النتائج أن خليط الخرسانة المضغوطة بالمدحلة الذي يحتوي على GGBS يتميز بطول العمر الافتراضي مقارنةً مع خرسانة الأسمنت البورتلاندي العادية، وأن قوة مخاليط GGBS تتحسن مع مرور الزمن وتوفر قوة ضغط أعلى مقارنةً مع خرسانة الأسمنت البورتلاندي العادية. وعلاوة على ذلك، أظهرت نتائج الاختبار أن خصائص قوة خليط الخرسانة المضغوطة بالمدحلة الذي يحتوي على GGBS تزيد عند استبدال الاسمنت البورتلاندي العادي بحبيبات خبث الفرن العالي المطحونة عند نسبة تصل إلى 40 ٪. وبينت مورفولوجيا SEM أيضا انتشار كثيف ومضغوط ومنتظم لهلام الكالسيوم – السيلكات – الهيدرات في خليط الخرسانة المضغوطة بالمدحلة الذي يحتوي على 40 % من GGBS.